Out-of-Plane Stability of Buckling-Restrained Braces

T. Okazaki
Hokkaido University, Japan

T. Hikino
Nippon Steel Engineering Co. Ltd.

K. Kajiwara
National Research Institute for Earth Science and Disaster Prevention, Japan

SUMMARY:
Large-scale shake table tests were performed at E-Defense to examine the out-of-plane stability of buckling-restrained braces (BRBs). Two planar specimens were subjected repeatedly to a near-fault ground motion with increasing magnitude. The specimens comprised a single-bay, single-story steel frame and a pair of BRBs placed in a chevron arrangement. The specimens were not braced at the brace-to-beam intersection in order to produce a condition where the BRBs were susceptible to out-of-plane instability. Standard BRBs were used in Specimen 1, while unique BRBs with a flexible segment at each end of the steel core were used in Specimen 2. Specimen 1 exhibited excellent behavior. As predicted by a simple buckling model, Specimen 2 failed due to out-of-plane buckling that involved severe kinking deformation at both ends of the steel core and severe twisting of the beam. The buckling model may be used to estimate minimal bracing requirements for steel frames with chevron BRBs.

Keywords: Shake table tests; Steel frames; Seismic design; Bracing; Lateral stability

1. GENERAL INSTRUCTIONS

The stable and predictable cyclic behavior of buckling-restrained braces (BRBs) has been demonstrated by numerous tests (e.g. Saeki et al. 1995; Black et al. 2004). However, recent large-scale, system-level tests indicate that the performance of BRBs can be affected significantly by interaction with the surrounding frame elements and detailing of the bracing connection. For example, tests by Mahin et al. (2004) and Roeder et al. (2006) suggest that local buckling and distortion of framing elements associated with large drifts can cause severe out-of-plane rotation of the gusset plates. Tests by Chou and Chen (2009) suggest that the stable inelastic behavior of BRBs can be compromised by out-of-plane buckling of the gusset plates.

Meanwhile, researchers in Japan including Tembata et al. (2004) and Takeuchi et al. (2004) noted the need to address out-of-plane stability of BRBs independently from framing action or gusset plate buckling. In particular, BRBs placed in a chevron arrangement (or "inverted-V" arrangement), as shown in Fig. 1(a), require special attention. In the U.S., the AISC Seismic Provisions (2005) require both flanges of the beam to be braced at the BRB-to-beam intersection unless the beam provides the required brace horizontal strength, P_{br}, and stiffness, β, defined as follows:

$$P_{br} = 0.01P_r \tag{1}$$

$$β = \frac{1}{0.75}\left(\frac{8P_r}{L_b}\right) \tag{2}$$

In the above equations, P_r is the required compressive strength of the BRB, L_b is the distance between the bracing point and point of intersection of the BRBs, and 0.75 is the resistance factor. Equations (1) and (2) express the nodal bracing requirement (AISC 2005) for the beam against a concentrated load delivered by the two BRBs, and do not address the out-of-plane stability of BRBs concerned in this paper.
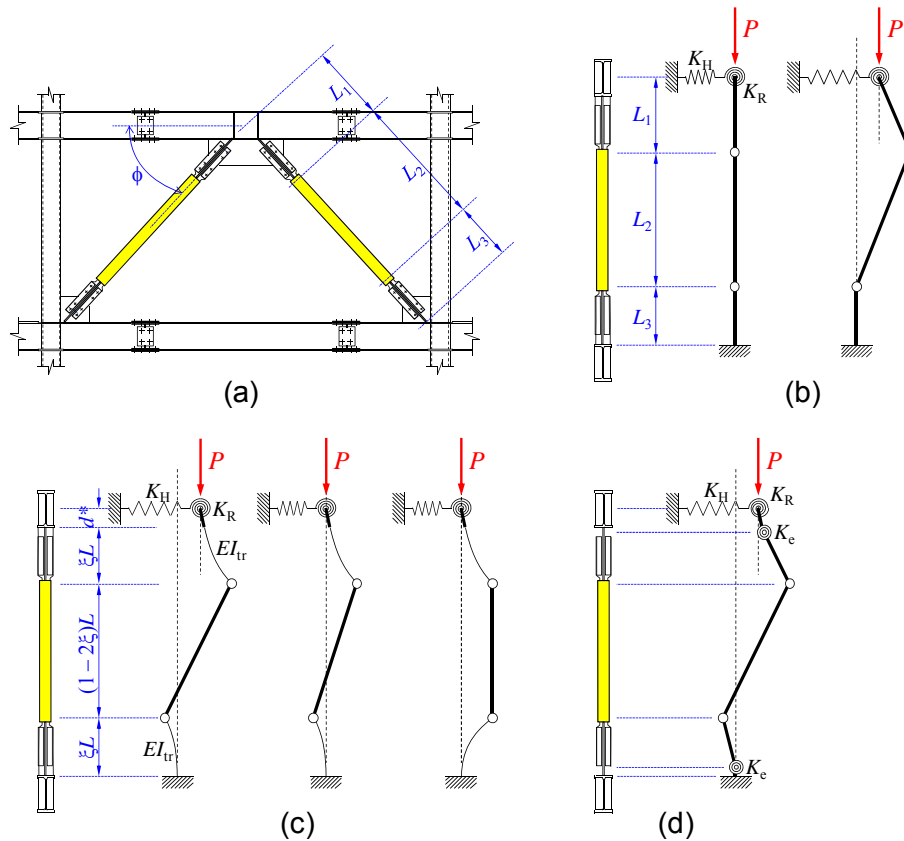
Figure 1. Out-of-plane stability model: (a) chevron brace; (b) model for standard connections; (c) model proposed by Kinoshita et al. (2007); and (d) model for alternative connections.

Previously, Tembata et al. (2004) and Kinoshita et al. (2007) derived a comprehensive set of analytical solutions to the out-of-plane stability problem of BRBs, and validated the solutions with static, cyclic loading tests. Takeuchi et al. (2004) and Kinoshita et al. (2008) investigated the rotational stiffness of BRBs and its bracing connections, respectively, acknowledging these stiffness values to be key factors that control the out-of-plane stability of BRBs. Koetaka and Kinoshita (2009) provide a review of the Japanese literature and propose general design criteria to control out-of-plane buckling of BRBs.

A research program was conducted to validate the design criteria proposed by Kinoshita et al. (2007) under a dynamic loading condition, and to examine how BRBs may behave after out-of-plane instability occurs. Large-scale shake table tests were conducted at E-Defense, a three-dimensional, large-scale earthquake testing facility maintained and operated by the National Research Institute for Earth Science and Disaster Prevention (NIED) of Japan. This paper describes a simplified version of the buckling model and summarizes the shake-table test program.

2. STABILITY MODEL

The following five assumptions are introduced to derive an analytical expression for the out-of-plane buckling strength of BRBs placed in a chevron arrangement as shown in Fig. 1(a).

1) Out-of-plane stability of BRBs is controlled by the forces and deformation produced in the plane that includes the BRB and that is perpendicular to the frame. The stability problem is not influenced by secondary in-plane framing action or tension in the opposite BRB.
2) The steel core of the BRBs includes short, unrestrained segments at the boundary between the yielding segment and the end stiffeners. The unrestrained segments have negligible flexural out-of-plane stiffness compared to any other segment of the BRB.
3) Yielding occurs only in the yielding segment of the steel core while all other components remain

elastic. Further, because of adequate stiffening, distortion of the gusset plates and the beam section is negligibly small.

4) The BRBs are adequately designed such that flexural buckling or local buckling of the steel core does not control the strength of the BRB.

5) Initial imperfection and out-of-plane drift is neglected.

Fig. 1(b) shows a first-order, out-of-buckling model of the BRB based on the above assumptions. The model is composed of rigid elements, internal hinges, and elastic end restrains. Internal hinges are placed in the steel core per assumption (2). The top end of the buckling model is the point of intersection between the BRB and the beam. The bottom of the system is modeled as rigid because the bottom represents the brace-beam-column node that is well braced. This model is a simplification of the elastic-perfectly plastic model proposed by Tembata et al. (2004) and Kinoshita et al. (2007), shown in Fig. 1(c).

Assumption (3) reflects the observation that Japanese engineers generally choose a bracing connection that restrain out-of-plane rotation. If the bracing connection is flexible, and thereby assumption (3) is not justified, then the alternative buckling model shown in Fig. 1(d) may be more adequate.

The model in Fig. 1(b) is used in this paper. Stability of this model is governed by the horizontal and rotational stiffness supplied at the top end of the BRB, K_H and K_R, and two length measurements L_1 and L_2. The spring constants may be evaluated based on the flexural and torsional stiffness of the beam and the properties of lateral braces placed at the BRB-to-beam intersection. As shown in Fig. 2(a), the buckling modes may be described in terms of three displacement parameters θ_1, θ_2, and u, of which two are independent. From the equilibrium condition, the critical load, P_{cr}, is determined as the smaller solution to the following quadratic equation.
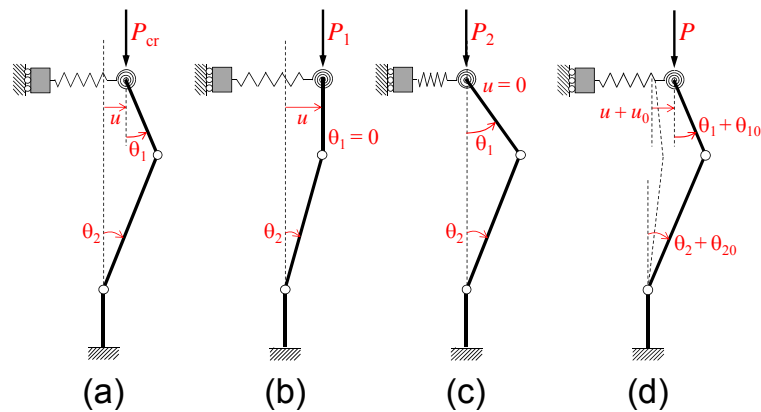
$$(P - P_H)(P - P_R) - P \cdot \left(\frac{L_1}{L_2} P_H\right) = 0 \tag{3}$$

In the above equation:

$$P_H = K_H \cdot L_2 \quad P_R = \frac{K_R}{L_1} \tag{4a, b}$$

Fig. 2(b) and (c) illustrate limit cases. For case 1, when the rotational spring is infinitely rigid ($\theta_1 = 0$, $u = L_2 \theta_2$), the critical load is $P_1 = P_H$. For case 2, when the translational spring is infinitely rigid ($u = 0$, $\theta_1/\theta_2 = L_2/L_1$), the critical load, P_2, is expressed as follows:

$$P_2 = P_R \frac{L_2}{L_1 + L_2} \tag{5}$$

Figure 2. Buckled configuration: (a) general mode; (b) limit case 1; (c) limit case 2; and (d) initial imperfection included.

The above solution is a special case of the solution derived by Kinoshita et al. (2007). Fig. 3 plots the combinations of P_1 and P_2 that achieves $P_{cr} = P_0$, where P_0 is the compressive strength of the steel core. The domain in the P_1–P_2 space above the curve and opposite the origin defines the safe domain where the buckling strength is greater than P_0, and thus out-of-plane buckling of the BRB may be avoided. The curves are plotted for $L_1/L_2 = 0.25$ and 0.5. The figure suggests that BRBs proportioned with larger bracing connections and shorter yielding segment requires somewhat larger restraints.

The buckling mode is derived from the same model as follows.

$$\frac{\theta_1}{\theta_2} = \frac{P_H}{P_R - P_{cr} + \frac{L_1}{L_2} P_H} = \frac{P_H - P_{cr}}{\frac{L_1}{L_2} P_H} \qquad (6a)$$

or

$$\frac{u}{L_1 \theta_1} = \frac{P_{cr}}{P_H - P_{cr}} \qquad (6b)$$

Figure 3. Condition to achieve $P_{cr} = P_0$

Equation (6) indicates that Case 1 dominates when P_2 is significantly greater than P_1 and thus $P_{cr} \approx P_1$, while Case 2 dominates when P_1 is significantly greater than P_2 and thus $P_{cr} \approx P_2$.

3. TEST PLAN

3.1. Specimens

Two braced frame specimens were tested in this program. Fig. 4(a) shows the specimen comprising a built-up wide-flange beam, two cold-formed square-HSS columns, and a pair of BRBs. The 4.15-m span and 2.10-m height corresponds to a 70%-scale building structure. After Specimen 1 was tested, the BRBs were replaced by a new pair of BRBs to prepare Specimen 2. The through-diaphragm detail was used to achieve rigid beam-to-column connections. The bracing connections adopted the standard Japanese detail that welds the fin plates directly to the beam. The beam was provided with stiffeners at the BRB-to-beam intersection to control local distortion of its web. The columns were rigidly connected to the shake table via stiff base beams. Table 1 lists the Japanese Industry Standards (JIS) designation and measured mechanical properties for each material used to fabricate the specimen. The specified minimum yield strength is 235, 295, and 325 MPa, respectively, for SN400, BCR295, and SM490 steel. The specimen was laterally braced along the columns and beam at discrete locations indicated in Fig. 2(a) by "×" marks. No bracing was provided at the middle segment of the beam (between points B and D) to intentionally reduce the torsional and translational restraint at the BRB-to-beam intersection.

The two specimens were nominally identical except for the BRBs. As shown in Figs. 4(b) and (c), the BRBs used a 74×12 mm plate for the steel core and a square-HSS 125×125×2.3 mm casing filled with mortar for the buckling-restraining system. Unlike commercialized BRB products, no capping plate was placed at either end of the casing. The key difference between the BRBs was the embedment length of the stiffened segment inside the steel casing. An experimental study by Takeuchi et al. (2009) suggest that, if the embedment length exceeds 1.5 to 2 times the depth of the core projection, then no local reduction in flexural stiffness occurs along the length of the steel core. While Specimen 1 met the minimum requirement suggested by Takeuchi et al. (Fig. 4(b) indicates 110 mm), Specimen 2 used a much shorter embedment length (Fig. 4(c) indicates 30 mm) to represent a least favorable BRB
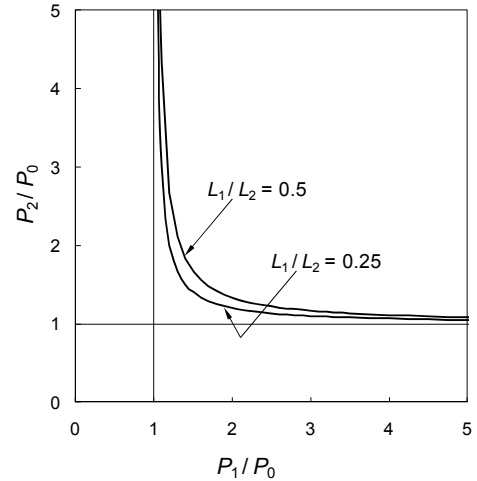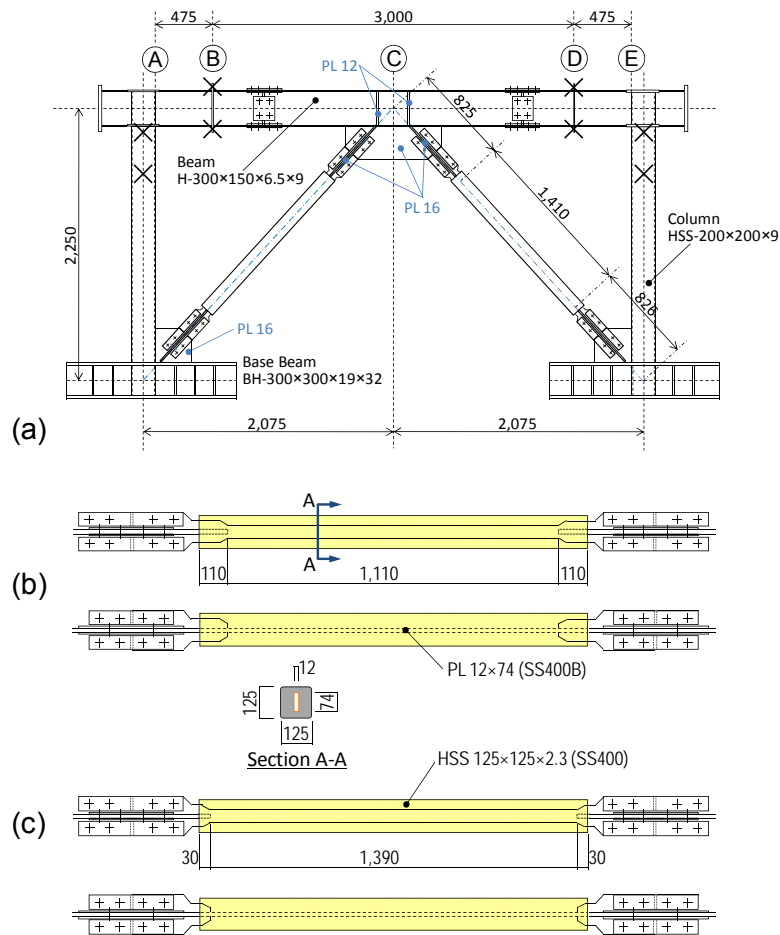
Figure 4. Test specimen: (a) elevation and out-of-plane bracing points; (b) BRBs in Specimen 1; and (c) BRBs in Specimen 2. (Dimensions in mm).

Table 1. Material properties

Material	JIS designation	Yield strength (MPa)	Tensile strength (MPa)	Elongation (%)
Steel core (12 mm)	SN400B	297	421	35
Beam flange (9 mm)	SN400B	327	456	27
Beam web (6 mm)	SN400B	376	472	29
Column (9 mm)	BCR295	434	518	19
Gusset plate (12 mm)	SM490A	315	441	32

design for out-of-plane stability. The BRBs were oriented with the flat plate steel core parallel to the plane of the frame. The parallel orientation is more commonly adopted than the orthogonal orientation, and represents a less favorable condition for out-of-plane stability of BRBs. Because rotational stiffness at the end of the BRB is developed by bearing between the stiffened segment and mortar, and the steel core itself possesses limited rotational stiffness, the shorter embedment length in Specimen 2 was expected to promote out-of-plane instability of the specimen. In other words, the stability model in Fig. 1(b) is valid for Specimen 2 but it is not valid for Specimen 1. Out-of-plane buckling of BRBs was not expected for Specimen 1.

Assuming that instability of the BRB would not occur, a simple, rigid-plastic analysis using the measured material properties estimated the lateral strength of the specimen to be 798 kN, at which stage the BRBs and underlying moment frame provide 58 and 42%, respectively, of the lateral strength

3.2. Stability design check

The spring constants K_H and K_R shown in Fig. 1(b) are determined by the weak-axis bending stiffness and torsional stiffness, respectively, of the beam. Elastic analysis assuming the beam to be simply supported at the intermediate bracing points (B and D in Fig. 4) and fixed at the face of the columns (A and E) for weak-axis bending and torsion, leads to K_H = 6,070 kN/m and K_R = 260 kN·m/rad. Using L_1 = 0.825 m and L_2 = 1.41 m (see Fig. 4), Equations (3) to (5) give P_1 = 8,560 kN, P_2 = 199 kN, and P_{cr} = 197 kN, While P_1 is substantially larger than the yield strength of the steel core based on the measured yield strength, P_y = 264 kN, P_2 and P_{cr} are smaller than P_y. Therefore, the stability model suggests the BRBs to buckle before developing their yield strength in compression, and suggests the buckling mode to be dominated by limit case 2.

Meanwhile, using P_r = 1.5P_y and L_b = 1.5 m, the minimal bracing requirements defined by Equations (1) and (2) is P_{br} = 3.9 kN and β = 2,810 kN/m. Because P_{br} is very easily exceeded by the weak-axis bending strength of the beam and K_H is more than double of β, the AISC Seismic Provisions do not require lateral bracing at the middle of the beam. In other words, neither specimen violates the stability requirements in the AISC Seismic Provisions.

3.3. Test procedure

The specimens were subjected to ground shaking at the E-Defense facility using the "test bed" system developed by Takeuchi et al. (2008). The test beds are multi-purpose devices that supply horizontal mass (69.4-metric ton for this project) to the specimen while adding minimal lateral force resistance. The specimen was attached to the test beds at the ends of the beams through pin-ended load cells. The test beds permitted only planar motion of the planar specimen. The test bed was also used to anchor the out-of-plane bracing indicated in Fig. 4(a). The scaling rules are summarized in Table 2 where λ indicates the scaling factor for length. For this test, λ = 0.7, and time and stress were not scaled.

The East-West component of the JR Takatori motion from the 1995 Kobe earthquake was introduced in the direction parallel to the primary plane of the specimen. This motion is characterized by a peak acceleration of 6.6 m/s² and strong velocity pulses. Fig. 5 shows the response acceleration spectrum obtained for 2 to 10% of critical damping (ζ = 0.02 to 0.1). The spectral response for ζ = 0.05 was between 17 and 23 m/s² for periods between 0.15 and 0.4 seconds, while the natural vibration period of the specimen was predicted as 0.2 sec. Therefore, the JR Takatori motion was twice as large as the design basis (Level 2) earthquake in Japan. The shake table tests were conducted by introducing the motion repeatedly with increasing amplification. Specimen 1 was tested with nine excitations between 14 and 120% of the JR Takatori EW motion. Specimen 2 was tested with seven excitations between 14 and 150% of the JR Takatori EW motion.

Table 2. Scaling rule

Parameters	Scaling Factor	
Length	λ	0.7
Mass	λ	0.7
Acceleration	λ	0.7
Time	1	1
Force	$λ^2$	0.5
Velocity	λ	0.7
Stress	1	1
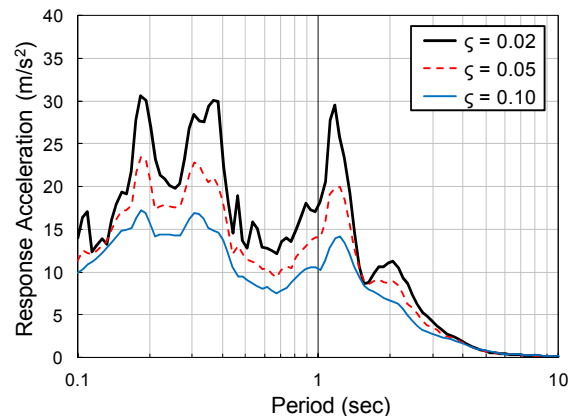
Figure 5. Response spectra for JR Takatori EW motion

3.4. Instrumentation

The load cells placed in the load path between the specimen and test beds were used to measure the story shear. Displacement transducers were used to measure the story drift and the out-of-plane deformation of beam and BRBs. The force distributions in the beam, columns, and BRBs were evaluated based on strain gauges placed at selected sections of the beam and columns. Elongation of the BRB steel core was measured from the change in relative distance between the end of steel casing and connection region of the steel core. Data was collected at a rate of 1,000 Hz. All data was passed through a low-pass filter to eliminate frequency content above 50 Hz.

4. TEST RESULTS

Based on unidirectional white noise excitation, the natural vibration period was determined as 0.18 sec for Specimen 1 and 0.19 sec for Specimen 2. The period was equivalent to that of a single or two story building. The damping ratio was evaluated as $\zeta = 0.03$. Damping was produced primarily by friction in the linear bearings supporting the test bed (Takeuchi et al. 2008).

Both specimens exhibited very similar response up to the 70% motion. Fig. 6 shows the story shear versus drift ratio response of the two specimens to the 100 and 120% motions. The drift ratio was evaluated as the relative displacement measured between the beam and column base divided by the story height of 2.1 m. Specimen 1 exhibited very stable and ductile behavior even under the largest 120% motion, developing a maximum drift of 0.014 radians and leaving a residual drift smaller than 0.001 radians. Minimal yielding was observed in the framing members after testing of Specimen 1 was completed. On the other hand, Specimen 2 experienced substantial degradation in elastic stiffness during motions 100% and larger, and recorded a maximum drift ratio of 0.016 radians during the 100% motion and 0.032 radians during the 120% motion. Fig. 7 shows the maximum drift and residual drift measured from each motion. Very similar response was obtained from the two specimens under motions up to 70%. The 100% and larger motions caused minimal damage to Specimen 1 but severe damage to Specimen 2. While the 150% motion produced extremely large drifts ranging between –0.06 and 0.025 radians, the residual drift after this motion was fairly small at –0.012 radians.

Fig. 8 shows photographs of Specimen 2 taken between the 120 and 150% motions. Fig. 8(a) views the elevation of the specimen from an angle. Kinking deformation is seen at the top and bottom ends of both BRBs, between the spliced gusset plate connection and steel casing. The kink rotation angle is notably larger at the top end of the BRB than at the bottom end, and the direction of kink rotation is opposite between the top and bottom. Permanent torsional deformation is seen in the beam. Fig. 8(b) is a close-up view of the middle portion of the beam and the top ends of the two BRBs. The close-up view indicates that the kinking deformation of the BRBs is accommodated by twisting of the beam. The deformation was dominated by rotation of the hinges and associated with negligible translation.
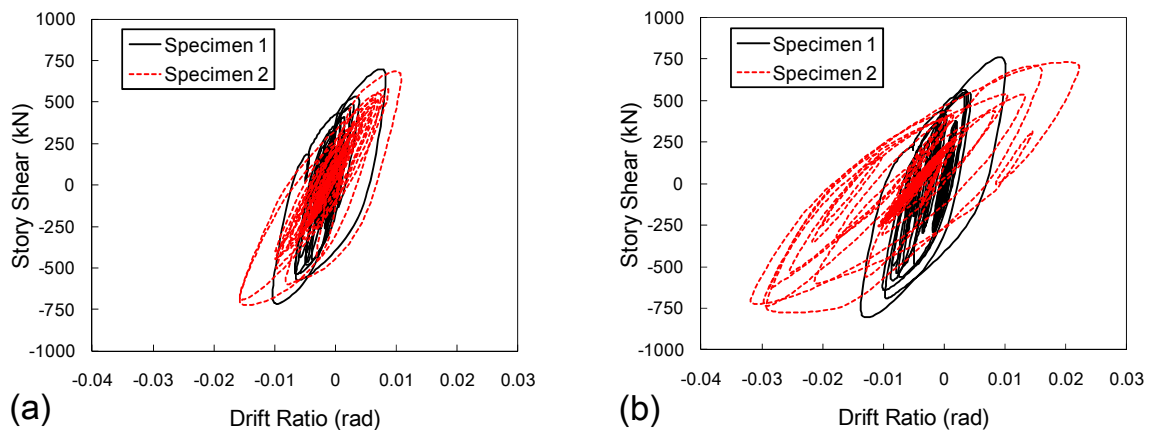

Figure 6. Frame response at: (a) 100% motion; and (b) 120% motion.
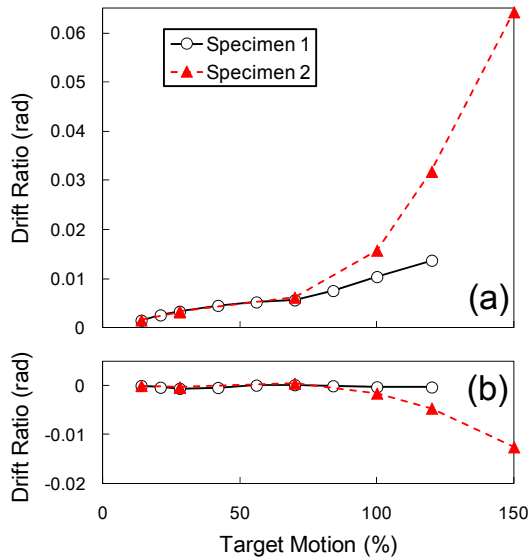
Figure 7. (a) Maximum drift; and (b) residual drift recorded at the end of each motion.

This deformation resembles the buckling mode for limit case 2 shown in Fig. 2(c). Although not visible in the photos, the steel casing was bulged outward at the side which the stiffeners bore against the steel casing. It is reminded that instability of Specimen 2 was promoted by lack of lateral restraint at the BRB -to-beam intersection and lack of out-of-plane rotational stiffness at both ends of the steel core.
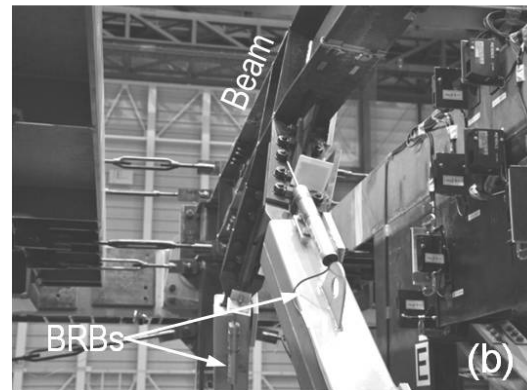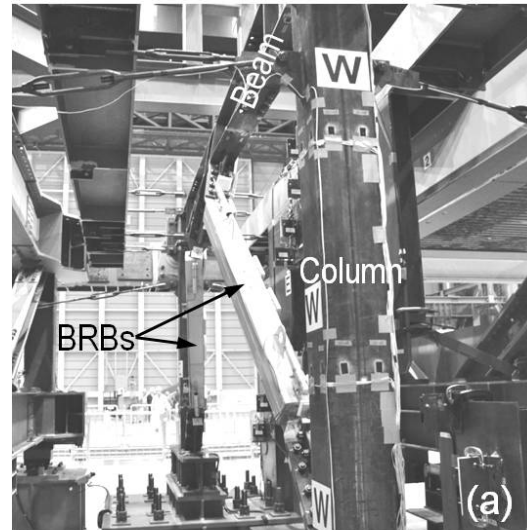

Figure 8. Specimen 2 after 120% motion: (a) side view; and (b) close-up view.

Fig. 9 further compares the two specimens from the 100% motion, plotting the elongation of the BRB steel core, and kink rotation at the top and bottom ends of the BRB, respectively, against the BRB tension. For Specimen 2, the figures indicate four time steps which correspond to instants when deformation increased rapidly. The response is shown for the West BRB which was placed on the closer side as viewed in Fig. 8. The behavior of the East BRB was roughly symmetric to the West BRB. Positive rotation is taken in the counter-clockwise direction as viewed in Fig. 8. The broken horizontal lines indicate the yield strength of the steel core based on the measured yield strength, P_y = 264 kN. The solid horizontal lines indicate the critical BRB strength, P_{cr} = 197 kN, which applies only to Specimen 2. The maximum measured tensile and compressive force was 1.24 and 1.19P_y, respectively, for Specimen 1 and 1.22 and 1.17P_y, respectively, for Specimen 2.

Fig. 9(a) shows that the stable cyclic performance expected of BRBs was observed in Specimen 1 but not observed in Specimen 2. In Specimen 1, the BRB steadily developed larger forces with elongation and produced minimal kink rotation in the BRB. On the other hand, the BRB in Specimen 2 developed severe out-of-plane deformation after exceeding its predicted buckling strength and yield strength. The compressive strength of Specimen 2 reduced substantially after undergoing two substantial compression excursions following Steps 1 and 3. Fig. 9(b) indicates that very large kink rotation formed at the top and bottom ends of the BRB, in opposite directions, and with the top end developing twice the rotation as the bottom. While residual kink rotation was present after the 70% motion, the 100% motion caused a very large residual rotation of 0.22 radians at the top and 0.09 radians at the bottom. Interestingly, the kink rotation increased in the same direction when the West BRB developed compression (Steps 1 and 3) and when the opposite East BRB developed compression (Steps 2 and 4). Therefore, it seems that the BRB in tension did not effectively control the out-of-plane instability of the BRB in compression.
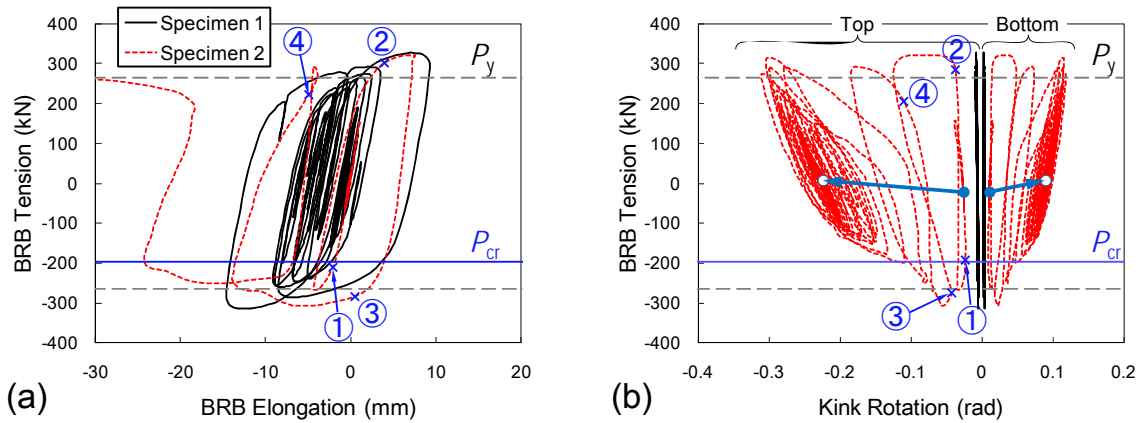
Figure 9. BRB response at 100% motion: (a) BRB elongation; and (b) BRB kink rotation.

Specimen 2 was subjected to two further motions after the 100% motion had caused severe buckling deformation to the BRBs. As plastic deformation accumulated in the beam and BRBs during the 100% and subsequent motions, the compressive strength of the BRBs gradually decreased. Meanwhile, the BRBs developed the same tensile strength that was developed during the 100% motion. After the 150% motion, the mortar was crushed at the end of the steel casing and the steel casing was deformed presumably due to the contact. However, no distress was found in the bracing connections. No fracture was visible in the steel core at the location of severe kinking deformation.

5. OBSERVATIONS

The buckling model shown in Fig. 1(b), which is a simplification of the original model proposed by Kinoshita et al. (2007) and shown in Fig. 1(c), predicted the out-of-plane buckling of BRBs in Specimen 2. Buckling deformation did not develop until the critical strength P_{cr} and the yield strength P_y was exceeded. The maximum measured BRB compression was $1.68P_{cr}$ for the East BRB and $1.56P_{cr}$ for the West BRB. Consequently, although the prediction was conservative, Equations (3) may be used to estimate the buckling strength for BRBs where the buckling model in Fig. 1(b) is justified. The local damage observed at the edges of the steel casing indicates that the steel core developed appreciable rotational stiffness as it bore against the buckling-restraining system. The rotational stiffness produced by this bearing mechanism may have contributed to the increase in buckling strength over the predicted strength P_{cr}.

Fig. 9(a) suggests that the stable inelastic behavior of BRBs was lost once buckling occurred. On the other hand, Fig. 6 shows that Specimen 2 maintained appreciable energy dissipation capacity during the 100 and 120% motions. After the BRBs had buckled, a large portion of the input energy was dissipated by the underlying moment frame and inelastic torsion of the beam, and less substantially by the BRBs. The secondary energy dissipation mechanism of the BRBF and the resiliency of the BRBs should be appreciated. However, considering that severe beam torsion can cause significant damage to nonstructural elements and the concrete slab, and makes replacement of BRBs impossible, the out-of-plane buckling deformation of BRBs demonstrated in Specimen 2 should be avoided.

6. CONCLUSIONS

Large-scale shake table tests were conducted to study the out-of-plane stability of BRBs placed in a chevron arrangement. Two chevron BRBF specimens were repeatedly subjected to a unidirectional ground motion with increasing amplification. In order to promote instability of the BRBs, no lateral bracing was provided at the BRB-to-beam intersection. While Specimen 1 used regular BRBs, Specimen 2 used BRBs with unusually short embedment length of the stiffened segment inside the steel casing. A simple buckling model was used to predict the out-of-plane buckling strength and

buckling mode of the BRBs. Key findings from this study are summarized in the following.

1) As predicted, the BRBs in Specimen 1 did not buckle. This specimen exhibited excellent seismic behavior. This result suggests that out-of-plane buckling of BRBs may be controlled by embedding the stiffened segment of the steel core sufficiently deep inside the steel casing.
2) Specimen 2 exhibited excellent behavior until the BRBs failed due to out-of-plane buckling. The buckling mode was as predicted by the buckling model. The measured BRB compression exceeded the predicted critical strength by 56 to 68% and exceeded the yield strength by 17 to 26%.
3) The resiliency of BRBs enabled stable energy dissipation of Specimen 2 even as the buckling deformation progressed to an extreme extent. Nonetheless, considering the damage expected to nonstructural elements and the concrete slab, out-of-plane buckling is not a preferred limit state for BRBs.

REFERENCES

American Institute of Steel Construction, Inc. (AISC). (2005). *Seismic Provisions for Structural Steel Buildings*. ANSI/AISC Standard 341-05. AISC, Chicago, Illinois.

Black, C.J., Makris, N., and Aiken, I.D. (2004). "Component testing, seismic evaluation and characterization of buckling-restrained braces." *Journal of Structural Engineering*, American Society of Civil Engineers, **130:6**, 880-894.

Chou, C.-C. and Chen, Pi-J. (2009). "Compressive behavior of central gusset plate connections for a buckling-restrained braced frame." *Journal of Constructional Steel Research*, **65**, 1138-1148.

Kinoshita, T., Koetaka, Y., Inoue, K., and Iitani, K. (2007). "Criteria of buckling-restrained braces to prevent out-of-plane buckling." *Journal of Structural and Construction Engineering*, Architectural Institute of Japan, **621**, 141-148, (in Japanese).

Kinoshita, T., Koetaka, Y., Inoue, K., and Iitani, K. (2008). "Out-of-plane stiffness and yield strength of cruciform connection for buckling-restrained brace." *Journal of Structural and Construction Engineering*, Architectural Institute of Japan, **632**, 1865-1873, (in Japanese).

Koetaka, Y. and Kinoshita, T. (2009). "Design criteria of buckling-restrained brace to prevent out-of-plane buckling." *Journal of Structural and Construction Engineering*, Architectural Institute of Japan, **641**, 1371-1378, (in Japanese).

Mahin, S., Uriz, P., Aiken, I., Field, C., and Ko, E. (2004). "Seismic performance of buckling restrained braced frame systems." *13th World Conference on Earthquake Engineering*, Paper No. 1681, Vancouver, British Columbia, Canada, August 1-6, 2004.

Roeder, C.W., Lehman, D.E., and Christopulos, A. (2006). "Seismic performance of special concentrically braced frames with buckling restrained braces." *8th U.S. National Conference on Earthquake Engineering*, San Francisco, California, April 18-22, 2006, Paper No. 1503.

Saeki, E., Maeda, Y., Nakamura, H., Midorikawa, M., and Wada, A. (1995). "Experimental study on practical-scale unbounded braces." *Journal of Structural and Construction Engineering*, Architectural Institute of Japan, **476**, 149-158, (in Japanese).

Takeuchi, T., Yamada, S., Kitagawa, M., Suzuki, K., and Wada, A. (2004). "Stability of buckling-restrained braces affected by the out-of-plane stiffness of the joint element." *Journal of Structural and Construction Engineering*, Architectural Institute of Japan, **575**, 121-128, (in Japanese).

Takeuchi, T., Kasai, K., Midorikawa, M., Matsuoka, Y., Asakawa, T., Kubodera, I., Kurokawa, Y., Kishiki, S., and Ando, H. (2008). "Shaking table test using E-Defense multipurpose test bed." *14th World Conference on Earthquake Engineering*, Beijing, China, October 12-17, 2008.

Tembata, H., Koetaka, Y., and Inoue, K. (2004). "Out-of-plane buckling load of buckling-restrained braces including brace joints." *Journal of Structural and Construction Engineering*, Architectural Institute of Japan, **581**, 127-134, (in Japanese).